*Biochimica et Biophysica Acta*, 602 (1980) 234—247


BBA 78971

# QUANTITATIVE ANALYSIS OF THE BINDING OF MELITTIN TO PLANAR LIPID BILAYERS ALLOWING FOR THE DISCRETE-CHARGE EFFECT

PETER SCHOCH and DAVID F. SARGENT

*Institut für Molekularbiologie und Biophysik, Eidgenössische Technische Hochschule, CH-8093 Zürich (Switzerland)*

(Received April 17th, 1980)

*Key words: Melittin; Lipid-protein interaction; Binding parameter; Surface potential; Discrete-charge effect; (Bilayer)*

## Summary

The interaction of melittin with lecithin bilayers was studied using the resulting surface potentials at the bilayer/water interfaces to monitor the association. Melittin added to the aqueous phase binds strongly to the interface but remains localized on that side of the bilayer to which it is added. The analysis of the binding curves reveals the inadequacy of the Gouy-Chapman theory for the fixed-charge surface potential in describing the electrostatic potential experienced by the adsorbed molecules. Calculations based on the Stern equation, modified for a discrete charge distribution, give a good fit to the experimental data. The thermodynamic analysis revealed different binding energies, $\Delta G^\circ$, at 10 and 100 mM ionic strength (−7.85 and −8.26 kcal/mol, respectively). Binding saturates at an area of 650 Å$^2$ per melittin molecule. A change in the surface dipole potential corresponding to −1.1 debye/$\epsilon_a$ ($\epsilon_a$ = dielectric constant of the adsorption region) had to be postulated. The Debye-Hückel length for a charge bound to the membrane/solution interface was found to be about one-third smaller than in bulk solution.

## Introduction

Polypeptide-lipid interactions are of great importance in many processes controlling the state of biological membranes. This report deals with the bilayer binding properties of melittin, a polypeptide of 26 amino acids, which we use to gain interesting insights into the thermodynamics of binding of

multiply charged peptides to neutral lipid membranes. In a second paper (unpublished results; for a preliminary report see Ref. 1) these insights are then applied to the analysis of a molecule showing more complicated binding properties, namely the polypeptide hormone, adrenocorticotropin-(1-24)-tetrakosipeptide ($ACTH_{1-24}$).

The primary structure [2] of melittin$^{6+}$, the main component (approx. 50% of dry weight) of bee venom, is:

(+)Gly-Ile-Gly-Ala-Val-Leu-Lys(+)-Val-Leu-Thr-Thr-Gly-Leu-Pro-Ala-Leu-Ile-Ser-Trp-Ile-
1 5 10 15 20

-Lys(+)-Arg(+)-Lys(+)-Arg(+)-Gln-Gln-$NH_2$
25

Its pronounced amphiphilic character is reflected in many of its properties, e.g., the strong surface activity [3—9]. Recently melittin was also shown to stimulate various phospholipases $A_2$ [10—12], one of which is a component of bee venom [13]. For a review of the biochemical and surface properties of melittin see Ref. 14.

Much work has been performed to establish the structural basis of melittin's mechanism of action. The amphiphilic structure of melittin cannot explain all of its effects: no simple correlation exists between lytic properties, surface activity and activation of phospholipases [15—17]. It is remarkable that both lysis and stimulation of phospholipases require a combined action of the whole molecule: neither the hydrophilic nor the hydrophobic part alone seems to have a significant effect.

From NMR and CD measurements [9,18—23] it has been suggested that in pure water, free melittin has predominantly an extended, flexible conformation, whereas binding to lipid structures or self-aggregation leads to a well defined conformational state that is quite different from that in solution. In the bound state, melittin seems to have a high $\alpha$-helix content, mainly in the N-terminal region. Its conformation is thus rather independent of the type of lipid or detergent and seems to be determined mainly by the apolar/polar interface of the lipid/water system [3,9]. NMR studies with detergent micelles [9,21] suggest that the entire hydrophobic portion of the molecule penetrates into the apolar lipid core, assuming a definite backbone conformation but retaining considerable rotational mobility of the side chains. The hydrophilic C-terminal part shows only weak interactions and probably conserves conformational mobility involving both backbone and side chains. It is usually assumed that melittin adsorbs only to the front side of the membrane, dipping more or less deeply into the lipid core without actually spanning it, but there is no proof of this as yet.

Using a recently developed method that detects electrostatic surface potentials (fixed-charge and dipole potentials) by their influence on membrane capacitance (capacitance minimization [24]), we have further characterized the interaction between melittin and planar lipid bilayers. The aim of this study was two-fold: (a) to check if part of the melittin molecule might be translocated to the opposite side of the bilayer upon binding, and (b) to work out the thermodynamic parameters that govern the binding of melittin to lecithin bilayers. This was carried out by analysis of the dependence of the

bilayer surface potential, caused by binding of the peptide, on ionic strength and bulk melittin concentration.

We first tried to fit the experimental data using the Stern equation [25,26], which uses the Gouy-Chapman fixed-charge surface potential to describe the energy barrier which is built up by charged adsorbants and impairs further adsorption. Such an approach was not sufficient to describe the experimental data, however, and we interpret the discrepancy in terms of discrete-charge effects [27]. From a discrete modelling of surface charges [28] we deduce a straight forward expression that relates the micropotential for a static array of bound charged molecules to the measured average surface potential. This expression allows us to modify the Stern adsorption equation to describe correctly the measured adsorption isotherms.

## Materials and Methods

Lecithin was isolated in a pure state (one spot on thin-layer chromatography) from egg yolks by alumina column chromatography as described in Ref. 29. The antoxidant, 2,6-di(*t*-butyl)-*p*-cresol (Sigma Chemical Co.) was added to the final solvent at 0.1% of the weight of the lipid. The fatty acid composition as determined by gas chromatography was 39.3% C16 : 0, 29.9% C18 : 1, 13.0% C18 : 2, 12.0% C18 : 0, 3,3% C20 : 4, 2.4% C16 : 1, with traces of C16 : 2.

The electrolytes usually contained 9 mM KCl and 2 mM Mes (2-(*N*-morpholino)ethanesulfonic acid, Fluka Chemicals), corresponding to an ionic strength of 10 mM; or 99 mM KCl with again 2 mM Mes (ionic strength 100 mM), both at a pH of 6.2. When the ionic strength was increased during an experiment it was performed by the replacement of an appropriate volume of solution by 4 M KCl. Changes of pH were performed by addition of small amounts of 0.1 M NaOH.

Melittin (*Apis mellifera*) was a gift from Dr. J. Lauterwein and was purified from lyophilized bee venom as described in Refs. 11 and 30. As shown by NMR [22], this melittin preparation is free of the $Gly^1$-formylated derivative, which is also a component of native bee venom. Thus, the melittin used in the present study is homogeneous with six positive charges per molecule.

Planar lipid bilayers were formed essentially by using the technique of Montal and Mueller [31]. Usually the bilayer was formed before all the hexane had evaporated from the surface monolayers. The resulting increase in bilayer compressibility facilitates the measurement of voltage-dependent capacitance.

The experimental set-up for the measurement of the capacitance minimization potential is shown schematically in Fig. 1. As the method has already been described in detail [24] only the principal aspects will be mentioned here. Artificial lipid bilayers can be compressed by an electric field: the minimal capacitance, $C_o$, is found only when the potential difference between the two surfaces is zero. Any asymmetry in surface potential, $\Delta\Psi$, caused for example by asymmetric binding of a charged substance, changes the capacitance-voltage characteristic: the minimum capacitance is shifted to $V = -\Delta\Psi$, where $V$ is the externally applied voltage. This potential, which thus minimizes $C_m(V)$, is called $V_{Cmin}$, and provides a measure of the amount of substance adsorbed.

All the experiments started with symmetrical conditions with respect to

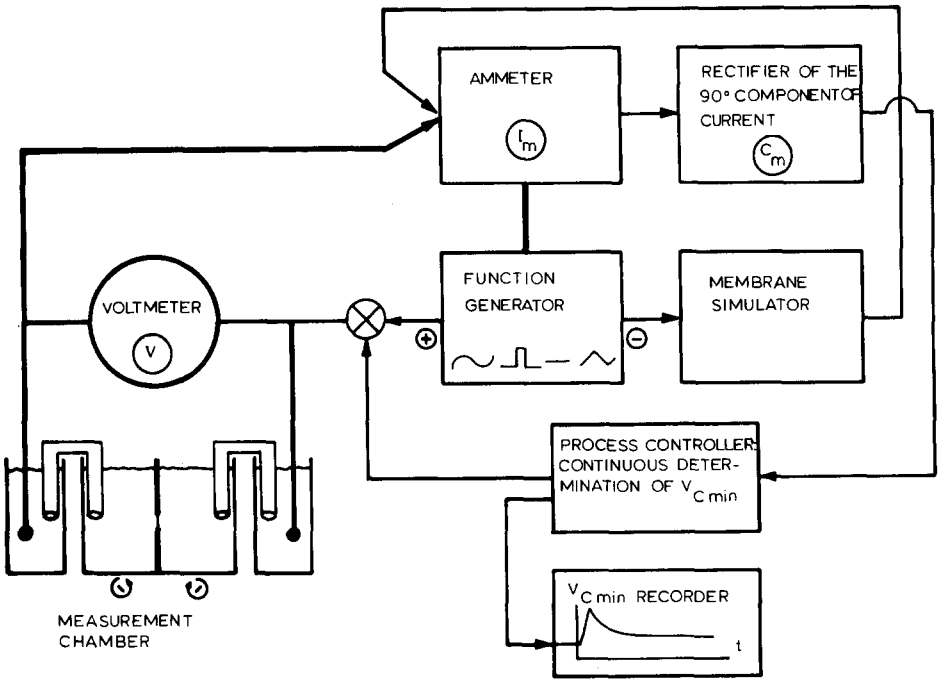


**Fig. 1. Block diagram of the experimental set-up. For a detailed description see Ref. 24. The element, $C_m$, rectifies the 90° current component of a small 1000 Hz signal and normalizes it with the applied amplitude. The membrane simulator (fed with an inverted signal) allows compensation of the constant part of the membrane capacitance signal to achieve better resolution. The process controller monitors the $C_m$ signal and applies a d.c. voltage to the membrane so that $C_m$ is minimized. This applied voltage is $V_{Cmin}$.**

lipid and aqueous solutions, i.e., with $V_{Cmin} = 0$. The change in surface potential found when a substance binds to a bilayer involves the Gouy-Chapman fixed-charge surface potential, $V_G$, and a dipole potential, $V_D$ (see Ref. 25). Therefore, $\Delta\Psi = -V_{Cmin} = \Delta V_G + \Delta V_D$ ($\Delta$ = difference between the two sides of the membrane). Only $V_G$ depends on the ionic strength in solution. This allows one to distinguish $V_G$ separately and thereby calculate the surface charge density and thus the amount of substance bound.

In our set-up, $V_{Cmin}$ is monitored continuously and the time course following addition of the peptide is plotted on a chart recorder.

## Results

*(a) Experimental data*

Fig. 2 demonstrates a typical experiment. It shows the time course of the development of the capacitance minimization potential, $V_{Cmin}$, upon addition of $2 \cdot 10^{-7}$ M melittin to the *cis*-side of the membrane, and the subsequent change of $V_{Cmin}$ when the ionic strength on either side of the membrane is increased. The initial rise of $V_{Cmin}$ represents the adsorption of melittin to the bilayer. The polarity is compatible with a deposition of positive charges on the front side of the membrane. The time course was not analyzed as it depends on stirring conditions.

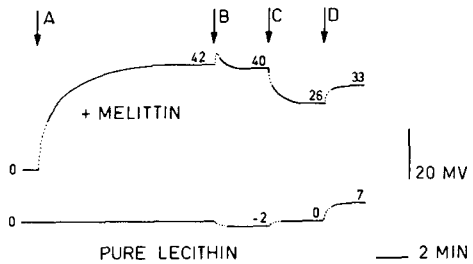


Fig. 2. Changes in $V_{Cmin}$ with time on addition of melittin. Time A, addition of melittin (final concentration 0.2 μM) to the *cis*-side of the bilayer. Time B, increase in the ionic strength on the *trans*-side from 10 to 90 mM by addition of KCl; the transient peak is observed whether or not the ionic strength is changed. Time C, increase in the ionic strength on the *cis*-side from 10 to 90 mM (addition of KCl). Time D, increase in the pH on the *trans*-side from 6.2 to about 8.5—9. The curve of pure lecithin represents the base-line for the melittin curve. During stirring the bilayer capacitance is difficult to measure and the corresponding portions of the curves are thus only approximate (dotted portions).

The 'pure lecithin' bilayer alone shows a slight response to changes in ionic strength. The minor change of 2 mV may be due either to the pure lipid itself (e.g., a small head-group reorientation) or be caused by minor impurities (e.g., free fatty acids): based on the Gouy-Chapman theory, a surface charge density of about one negative charge per 23 000 Å$^2$ would suffice to explain the observed shift. As will become evident in the next section, the electrical effects of such a low background surface charge density will be overshadowed by bound melittin at a bulk melittin concentration of only $3 \cdot 10^{-9}$ M (see Fig. 5), and can thus be neglected. In any case, the changes in $V_{Cmin}$ values for melittin-containing membranes are analyzed relative to the corresponding portion of the curve for the unmodified bilayer and thus reflect only changes caused by the presence of melittin itself.

After $V_{Cmin}$ reached equilibrium (42 mV), the ionic strength was increased

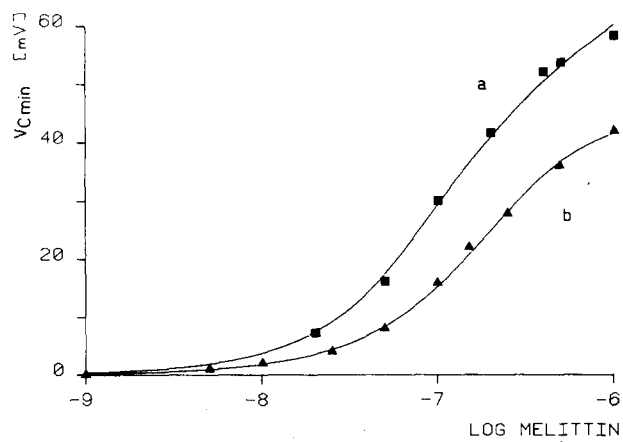


Fig. 3. The binding curves of melittin to egg lecithin bilayers at two different ionic strengths. (a) 0.01 M KCl, (b) 0.1 M KCl, pH 6.2. The standard deviation of the individual data points is 1.4 mV. The solid line is the theoretical curve drawn with the parameters given in Table I according to the modified Stern equation.

on the *trans*-side. The small decrease (2 mV) in $V_{Cmin}$ is identical to that found for the native bilayer, thus no charges resulting from the binding of melittin have appeared on the *trans*-side. When the salt concentration was raised on the *cis*-side, $V_{Cmin}$ decreased by 14 mV or, taking the change of the base-line into account, by 16 mV. This change is caused by the increased shielding of the positive surface charge of melittin by the higher ionic strength. A quantitative description of this change must also reflect the fact that lowering the surface potential reduces the electrochemical potential of bound charged molecules, which in turn allows more molecules to enter the adsorption plane from the aqueous solution.

At the end of the recording, the pH in the *trans*-chamber was increased from 6.2 to 8.5—9.0. The observed change of $V_{Cmin}$ is again clearly only that of the unmodified bilayer. The polarity implies that negative charges were created by deprotonation. This again could be caused by fatty acid impurities. The 7 mV change would correspond to a density of about one charge per 3300 Å$^2$.

Fig. 3 shows the 'binding curves' of melittin to lecithin bilayers at two different ionic strengths. (Although the term binding is not entirely correct (the value of $V_{Cmin}$ itself rather than the surface concentration is plotted), we will use it here in this context.) Binding becomes measurable between $10^{-9}$ and $10^{-8}$ M melittin. This is much lower than the limit of detection reported for all other lipid-melittin studies. The upper limit of measurement is given by the lytic effect of melittin: above about $10^{-6}$ M melittin, bilayers are too short-lived for meaningful measurements.

*(b) Thermodynamic analysis of the binding curves; indication of discrete-charge effects*

Discrete-charge phenomena in adsorption processes are reflected in the so-called Esin-Markov coefficient [27]. This coefficient is related to the change in the mean fixed-charged surface potential, $V_G$, for a 10-fold increase in the aqueous concentration of the free adsorbent, $c_f$: $dV_G/d\log c_f$. If adsorption is determined purely by the Gouy-Chapman theory this coefficient is expected to be at most 58 mV/$z$ ($z$ = charge of adsorbent, see Appendix A). A larger value is traditionally ascribed to discrete-charge effects. The reason is simple to understand: if the electrostatic potential at the adsorption plane is not uniform but varies locally according to the discrete nature of the bound charges, then the newly adsorbing molecules would sit into the wells in the micropotential, thereby maximizing the nearest-neighbour distance. As it is this micropotential ($V_{eff}$) that determines the adsorption, more molecules may bind than expected from the macroscopically measured $V_G$. For melittin with $z = 6$ the Gouy-Chapman theory suggests a slope of about 10 mV/decade.

The observed slope (Fig. 3) is about 40 and 33 mV/decade for the two ionic strengths, respectively. That in itself does not prove the existence of discrete-charge effects, as $V_{Cmin}$ also has a dipole contribution. However, as a first approximation, the observed slope strongly suggests the influence of the discreteness of adsorbed melittin and, as the analysis will show, it is even more marked than the slope of $V_{Cmin}$ suggests.

*(c) Binding model and fitting of the binding curves*

$V_{Cmin}$ is composed of $V_G$ and $V_D$, the changes in the surface potentials upon binding. $V_G$ has been explicitly shown to be associated solely with the *cis*-side (no *'trans'* effect) and, considering the geometry of adsorption, this is also assumed for $V_D$, although this is not crucial to the analysis. Both $V_G$ and $V_D$ are functions of $c_b$. The $V_{Cmin}$ vs. $c_b$ curves were fitted to Eqn. 1:

$$-V_{Cmin} = V_G + V_D = \frac{2RT}{F} \ln(s + \sqrt{s^2 + 1}) + \frac{D}{\epsilon_a} \cdot \frac{c_b}{\epsilon_0} \tag{1}$$

with

$$s = z \cdot F \cdot c_b / \sqrt{8 \cdot [KCl] \cdot \epsilon_o \epsilon \cdot RT} \tag{2}$$

where $\epsilon_a$ = dielectric constant of the adsorption layer, $\epsilon$ = dielectric constant of the aqueous solution, and $D$ = change of dipole moment per bound molecule. The other symbols have their usual meanings. $V_G$, the average potential at the surface of the membrane relative to the bulk solution, is assumed to be given by the Gouy-Chapman equation for 1-1 electrolytes [25,26]. (As $V_{Cmin}$ depends on the average potential, the use of the Gouy-Chapman theory is justified.) $V_D$ is the effective potential jump at the interface caused by the adsorbed molecular dipoles [26].

Melittin is known to aggregate in aqueous solution, dependent on both ionic strength and concentration. Under the conditions of the present measurements, however, melittin occurs exclusively in the monomeric form, as shown recently by fluorescence [32] and NMR [23] studies. Other studies indicate that melittin binds as the monomer [9,11]. The description of the system is thus simplified considerably.

To express the surface concentration of bound melittin, $c_b$, as a function of the free concentration, $c_f$, the Stern adsorption isotherm [25] was modified for discrete-charge effects by substituting $V_G$ with $V_{eff} = V_G \cdot \gamma$, where $\gamma$ is derived from a theoretical description of the potential profile around a bound surface charge (see Appendix B). The modified Stern equation has the following form:

$$c_b = \frac{c_f}{c_f^o} (c_{bmax} - c_b) \exp\left(-\frac{\Delta G^\circ + zFV_G\gamma}{RT}\right) \tag{3}$$

for which $c_f^o$ = standard concentration in free solution ≡ 1 M, $c_{bmax}$ = saturating surface concentration, and $\Delta G^\circ$ = change in the standard free energy. The standard state for bound melittin corresponds to the value at half-maximal saturation.

It has to be emphasized that $\Delta G^\circ$ includes the energy difference per mol between the two standard states but excludes any intermolecular electrostatic interactions of bound molecules. Included in $\Delta G^\circ$ are intermolecular interactions in solution, if present (we have not explicitly introduced activity coefficients), and changes in intramolecular interactions upon binding. For this reason, $\Delta G^\circ$ may be expected to vary with the KCl concentration.

The data of the two binding curves (Fig. 3) were fitted to the adsorption isotherm (Eqn. 3) by a least-squares method. Only $\Delta G^\circ$ was allowed to depend implicitly on the KCl concentration. Table I shows the numerical results.

TABLE I

THERMODYNAMIC PARAMETERS FOR THE BINDING OF MELITTIN TO LECITHIN BILAYERS ACCORDING TO THE MODIFIED STERN EQUATION

The values in parentheses are standard deviations found by the ($\chi^2_{min}$ + 1)-method [38]. They represent the uncertainties introduced by that parameter with which the numerical coupling is strongest and are therefore only indicative of the total uncertainty.

| | |
|---|---|
| $\Delta G^o$ (0.01 M KCl) (kcal/mol) | −7.85 (−0.25, +0.15) |
| $\Delta G^o$ (0.1 M KCl) (kcal/mol) | −8.26 (−0.25, +0.15) |
| $1/c_{bmax}$ (Å$^2$/molecule) | 650 (−130, +220) |
| $\kappa_o^{-1}$ * (Å · M$^{1/2}$) | 1.99 (−0.07, +0.05) |
| $D/\epsilon_a$ (debye) | −1.10 (−0.06, +0.05) ** |

* See Discussion.

** Polarity of dipoles: membrane side negative.

Figs. 4 and 5 show some theoretical curves drawn with the parameters given in Table I. The concentration range chosen is not limited to that of the present experiments, but is extended to the range usually used in work on the physiological mechanism of melittin.

The actual Esin-Markov coefficients may be determined from curves 1b and 2b of Fig. 4, as they do not include dipole contributions: the coefficients amount to about 46 and 57 mV per decade of free melittin at 0.01 and 0.1 M KCl, respectively. These values clearly argue for the existence of pronounced discrete-charge effects.

The fixed-charge surface potentials (curves b) diverge less than the total surface potentials (curves a), as the increased binding is partially shielded by the electrolyte. The different degree of binding at the two ionic strengths is more obvious in the $V_{Cmin}$ curves, although the increased binding at higher ionic strength results in a reduction of $V_{Cmin}$ because the dipole contribution

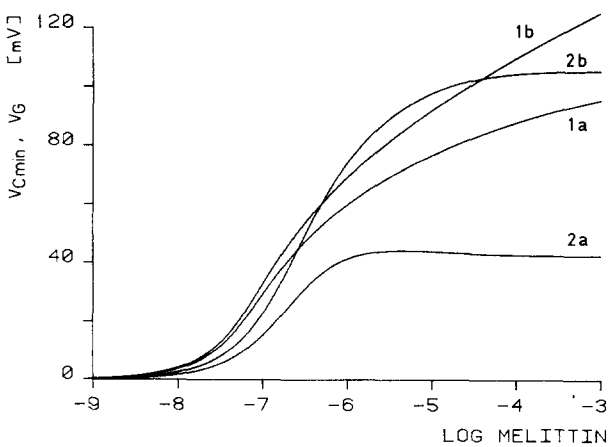


**Fig. 4. Theoretical curves of surface potentials at the lecithin/solution interface for adsorption of melittin (parameter values given in Table I). Abscissa, molar concentration of aqueous melittin (assuming no aggregation). Curves 1, 0.01 M KCl; curves 2, 0.1 M KCl; curves a, $V_{Cmin}$; curves b, $V_G$. The differences between curves 1a and 1b or 2a and 2b correspond to dipole potential changes, $V_D$.**

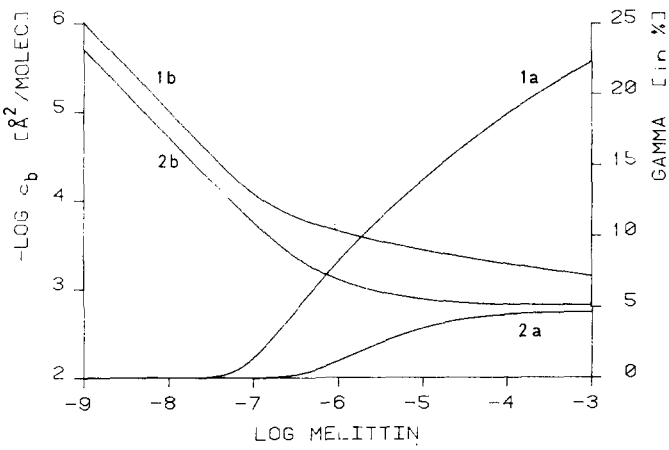


Fig. 5. Theoretical curves for melittin-lecithin binding (parameter values given in Table I). Abscissa, molar concentration of aqueous melittin (assuming no aggregation ). Curves 1, 0.01 M KCl; curves 2, 0.1 M KCl; curves a, $\gamma$ (= gamma); curves b: $-\log c_b$.

is negative. A further point of interest is the very different melittin concentrations at which saturation is reached: $10^{-5}$ M at 0.1 M KCl, but about four orders of magnitude higher at 0.01 M KCl.

## Discussion

It was necessary to consider discrete-charge effects to explain the steep rise in $V_{Cmin}$ with increasing melittin concentration (Esin-Markov coefficient). To this end we modified the original Stern equation with a discreteness factor, $\gamma$ (Eqn. B4), reflecting the reduction of mutual repulsion between bound, charged molecules. It stems from a simple model of the potential profile around a surface charge, yet leads to a good description of the binding data.

Before discussing the quantitative results, we wish to comment on the basic geometry of the melittin-bilayer interaction. The independence of $V_{Cmin}$ of the ionic strength on the *trans*-side of the bilayer shows that no charge appears on that side. This means that neither melittin as a whole nor any charged part of it crosses the bilayer: both ends of the molecule are presumably 'anchored' on the *cis*-side. Accepting some $\alpha$-helical content of bound melittin [9,21] and resulting restrictions on length, it is unlikely that any part of the molecule would be exposed on the *trans*-side. This is consistent with the structure proposed in Ref. 18.

Our thermodynamic analysis assumes that each bound melittin deposits six positive charges right at the membrane/solution interface (if charges were displaced into the aqueous solution by a distance comparable with $\kappa^{-1}$, the surface potential would be considerably reduced). Indeed, our experimental data are better fitted with $z = 6$ than with $z = 5$ or less. Further supporting evidence comes from NMR studies with melittin bound to detergent micelles, from which it appears that the three lysines, two arginines and Gly[1] are all positively charged below pH 7 and lie probably in the interfacial region of the

micelle (Refs. 9 and 21; and Brown, L.R., personal communication).

The thermodynamics and electrostatics of adsorption are well described by the Stern equation modified to consider discrete-charge effects. However, we also tried to fit the binding data (Fig. 3) to a simpler adsorption isotherm neglecting the limitation of the binding process by spatial restrictions on the membrane surface: this results in the $(c_{bmax} - c_b)$ term of Eqn. 3 being replaced by a constant factor. As long as $c_b$ is small, a reasonable fit to the data is also obtained (not shown), but deviations are visible at the higher ionic strength (0.1 M KCl) at $c_f > 10^{-7}$ M.

Several aspects of the fitted parameters (Table I) deserve comment:

(1) *Binding energies.* The difference of the binding energies at the two ionic strengths, which is small but in our opinion significant, indicates that binding is favored at the higher ionic strength (the dissociation constants differ by a factor of 2). The explanation must lie in intramolecular interactions as intermolecular repulsions are absent in solution (distances too large) and are explicitly taken into account when bound to the membrane.

(2) *Maximal surface concentration.* There are two alternative interpretations of the origin of the limited binding capacity. $1/c_{bmax}$ = 650 Å$^2$/molecule could be the area of the adsorbed melittin molecules themselves, but this seems improbable as the whole molecule would have to be spread flat on the membrane/solution interface. Alternatively, 'bound' lipid may contribute to the area of the binding site: about 10 lipid molecules would already result in the observed area. This number of associated lipid molecules has been suggested by other studies [33,34]. The relatively large uncertainty in $1/c_{bmax}$ results from the small degree of saturation attainable (Fig. 3). $c_{bmax}$ cannot be determined at all from the curve at 0.01 M KCl. The value of 650 Å$^2$ per melittin molecule together with its uncertainty originates from the binding curve at 0.1 M KCl where the highest surface concentration reached is about one molecule per 1270 Å$^2$.

(3) *Debye-Hückel length at a charged surface.* We define $\kappa_o$ as the reciprocal Debye-Hückel length for a 1 M 1-1 electrolyte and, following the original Debye-Hückel theory for ions in solution, assume that $\kappa = \kappa_o^{-1}\sqrt{[KCl]}$, where [KCl] is the bulk concentration. In solution, $\kappa_o^{-1}$ has the value of 3.04 Å. In the present case, for charges bound to a low-dielectric surface, it assumed a value about 1/3 smaller than in bulk solution, which means that the potential around a surface charge decays faster than in free solution. This is not unreasonable, as a charge at the interface to a medium of low dielectric constant produces a higher potential than in solution [28], which will result in a denser cloud of counterions, thereby reducing the Debye-Hückel length. This would explain the stronger dependence of the free energy on ionic strength for the bound compared to the dissolved melittin (see paragraph 1, above).

(4) *Change of the surface dipole moment per bound melittin molecule.* The data cannot be fitted by the model presented if no dipole component is included. Many factors could contribute to the value, e.g., the normal component of any dipole moment of melittin itself, plus any rearrangements of phospholipid and surface water molecules. The effective dipole moment is given formally by the fraction, $D/\epsilon_a$, for which the value of —1.1 debye was

found. If $\epsilon_a = 10$, then $D$, the change of the dipole moment per bound melittin, is about - 11 debye. Considering that even a single peptide bond has a value of 3.71 debye [35], our value of about 11 debye per bound melittin molecule is quite modest. This is easily rationalized on the basis of partially compensating or tangentially oriented dipoles.

## Appendix A

*The Esin-Markov coefficient for a multiply charged absorbent*

Taking the effective local potential, $V_{eff}$, into consideration, the Esin-Markov coefficient is computed as follows (cf. Ref. 27). In the lower range of the binding curve, where $c_{bmax}$ does not yet noticeably limit the binding process, the surface charge density, $\sigma$, may be expressed by:

$$\sigma = z \cdot F \cdot c_b = k \cdot z \cdot c_f \cdot \exp(-zFV_{eff}/RT) \tag{A1}$$

where $k$ is a combination of constant terms, as may be deduced from Eqn. 3.

For a 1-1 electrolyte in the range of small fixed-charge surface potentials, $FV_G << 2RT$, the Gouy-Chapman theory allows the linear approximation:

$$\sigma = \alpha \cdot V_G \tag{A2}$$

Combining Eqns. A1 and A2 yields, after suitable manipulation:

$$\frac{dV_G}{d \ln c_f} = V_G \cdot \left(1 - \frac{zF}{RT} \cdot \frac{dV_{eff}}{d \ln c_f}\right) \tag{A3}$$

Replacing $dV_{eff}/d\ln c_f$ by $(dV_{eff}/dV_G) \cdot (dV_G/d\ln c_f)$ and rearranging leads directly to the Esin-Markov coefficient:

$$\frac{dV_G}{d \log c_f} = \frac{2.3RT/zF}{(RT/zFV_G) + (dV_{eff}/dV_G)} \tag{A4}$$

Two special cases are of interest: (1) $dV_{eff}/dV_G = 0$ (discreteness and very low adsorption):

$$\frac{dV_G}{d \log c_f} = 2.3V_G \tag{A5}$$

and (2) $dV_{eff}/dV_G = 1$ (uniform distribution) and $zFV_G >> RT$ (high adsorption):

$$\frac{dV_G}{d \log c_f} = 58.4 \text{ mV}/z \tag{A6}$$

which represents the maximal slope consistent with the Gouy-Chapman theory.

## Appendix B

*The discreteness factor $\gamma$ for point surface charges*

With a discrete surface charge distribution the adsorption of a charged species is determined by the effective local potential. In contrast to recent attempts to account for this phenomenon in the adsorption of hydrophobic

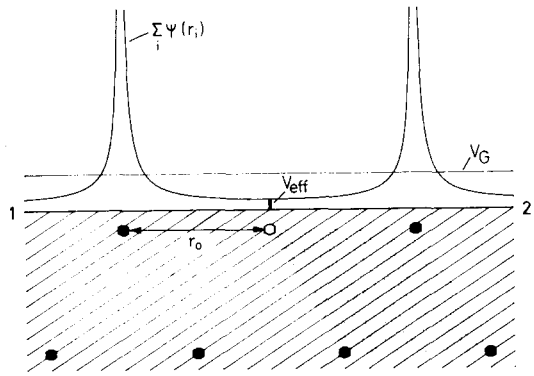


Fig. 6. Schematic representation of the discrete nature of the membrane surface. Lower half, hexagonal array of adsorption sites on the membrane surface. Upper half, the local potential $\Sigma_i \psi(r_i)$ along the line 1—2. •, occupied site; ○, free adsorption site. $V_{eff}$, the actual potential that determines the adsorption to free adsorption site. $V_G$, average potential along the interface as given by the Gouy-Chapman theory or by an analytical averaging of the discrete potential profiles. $r_o$, distance to nearest neighbors in the hexagonal arrangement of bound molecules.

ions to internal binding sites [36,37], we consider the case of charges directly on the aqueous/hydrophobic boundary, and include in the calculations an explicit description for shielding by the adjacent diffuse layer. Fig. 6 illustrates the quantities dealt with in this section.

The potential in the adsorption plane around a fixed point charge is given by the following expression [28]:

$$\psi(r) = \frac{a}{r} \exp(-r\kappa) \tag{B1}$$

where $r$ is the distance from the fixed charge and lies along the interface, $\kappa$ is the reciprocal Debye-Hückel length and $a$ is a combination of various constants (containing, among other terms, the magnitude of the charge, $z$, and the dielectric constants of the membrane and the aqueous solution, $\epsilon_m$ and $\epsilon$: $a = z \cdot 353$ Å $\cdot$ mV for $\epsilon = 79.4$ and $\epsilon_m = 2.1$).

The interactions of a charge $q = ze$ embedded in a hexagonal array with separation $r_o$ are approximated by considering only the six nearest neighbors forming a hexagon around $q$. This approximation is valid as long as $r_o >> \kappa^{-1}$, the error being about 1% for $r_o = 5.6 \cdot \kappa^{-1}$ and about 10% for $r_o = 2.8 \cdot \kappa^{-1}$. The total potential from these six nearest neighbors is:

$$V_{eff} = 6 \frac{a}{r_0} \exp(-r_0\kappa) \tag{B2}$$

In principle, this expression could be used to describe the discrete-charge effects in adsorption. However, to get a more illustrative factor we define $\gamma = V_{eff}/V_A$, where $V_A$ is the average fixed-charge surface potential, often referred to as macropotential. For smeared surface charges $V_A$ is given by the Gouy-Chapman theory, but for a distribution of discrete charges we deduce it by averaging Eqn. B1 over the area/molecule:

TABLE II

A NUMERICAL COMPARISON OF $V_G$ AND $V_A$

| $c_b^{-1}$ (Å$^2$/melittin$^{6+}$) | $V_G/V_A$ | |
|---|---|---|
| | 0.01 M KCl | 0.1 M KCl |
| $10^6$ | 1.55 | 1.55 |
| $10^5$ | 1.55 | 1.55 |
| $10^4$ | 1.42 | 1.53 |
| $5 \cdot 10^3$ | 1.20 | 1.49 |
| $2 \cdot 10^3$ | 0.80 | 1.29 |
| $10^3$ | 0.53 | 1.01 |
| 650 | 0.40 | 0.82 |

$$V_A = \frac{\int_0^\infty \psi(r) \cdot 2\pi r \cdot dr}{\text{area per charge}} = \frac{\int_0^\infty 2\pi a \cdot \exp(-r\kappa) \cdot dr}{\sqrt{3}/2 \cdot r_o^2} = \frac{4\pi a \kappa^{-1}}{\sqrt{3} \cdot r_o^2} \quad \text{(B3)}$$

Combining Eqns. B2 and B3 yields:

$$\gamma = V_{eff}/V_A = \frac{3\sqrt{3}}{2\pi} r_0 \kappa \cdot \exp(-r_0 \kappa) \quad \text{(B4)}$$

In Eqns. 1—3 the average surface-charge potential is given by the Gouy-Chapman theory. Our modification of the Stern equation (Eqn. 3) consists of setting $V_{eff} = \gamma \cdot V_G$, which implies the equality of $V_G$ (derived from the Gouy-Chapman theory) with $V_A$ as obtained above. A numerical comparison of $V_G$ and $V_A$ (Table II) shows that, in the range of our binding data, $V_{eff}$ as used in Eqn. 3 is up to 55% larger that it would be according to Eqn. B2. Our value for $V_{eff}$ is clearly only approximate, but it represents a first step in the description of interactions of discrete charges on a surface.

This derivation of $\gamma$ assumes point charges of valence $z$, which is of course inadequate. First, the $z$ charges are distributed along the melittin molecule. An error is introduced by calculating $V_{eff}$ from the distance between the centers of the hypothetical point charges instead of between the distributed charges. This may lead to serious deviations as soon as the intermolecular separation is comparable with the intramolecular spacing. The fact that four of the six charges are found on consecutive amino acid residues (Nos. 21—24) reduces this danger, however.

A second objection is the finite size of the individual charges. At high surface concentrations and especially high ionic strengths, a distance of closest approach, $R$, should be introduced.

## Acknowledgements

This work was supported by grants from the Swiss National Science Foundation and the Swiss Federal Institute of Technology to Professor R. Schwyzer, Head of this research group. We are grateful for his interest and advice. Thanks are due to Miss R. Kuhn and Mrs. D. Sargent for typing the manuscript.

## References


1 Schoch, P., Sargent, D.F. and Schwyzer, R. (1979) Biochem. Soc. Trans. 7, 846—849
2 Habermann, E. and Jentsch, J. (1967) Hoppe-Seyler's Z. Physiol. Chem. 348, 37—50
3 Sessa, G., Freer, J.H., Colacicco, G. and Weissman, G. (1969) J. Biol. Chem. 244, 3575—3582
4 Dufourcq, J. and Faucon, J.F. (1977) Biochim. Biophys. Acta 467, 1—11
5 Mollay, C. and Kreil, G. (1973) Biochim. Biophys. Acta 316, 196—203
6 Knoeppel, E., Eisenberg, D. and Wickner, W. (1979) Biochemistry 18, 4177—4181
7 Habermann, E. (1958) Z. Exp. Med. 130, 19—23
8 Habermann, E. and Reiz, K.G. (1965) Biochem. Z. 343, 192—203
9 Lauterwein, J., Boesch, C., Brown, L.R. and Wuethrich, K. (1979) Biochim. Biophys. Acta 556, 244—264
10 Mollay, C. and Kreil, G. (1974) FEBS Lett. 46, 141—144
11 Mollay, C., Kreil, G. and Berger, H. (1976) Biochim. Biophys. Acta 426, 317—324
12 Shier, W.T. (1979) Proc. Natl. Acad. Sci. U.S.A. 76, 195—199
13 Neumann, W. and Habermann, E. (1954) Arch. Exp. Pathol. Pharmakol. 222, 367—387
14 Habermann, E. (1972) Science 177, 314—322
15 Habermann, E. and Kowallek, H. (1970) Hoppe-Seyler's Z. Physiol. Chem. 351, 884—890
16 Schroeder, E., Luebke, K., Lehmann, M. and Beetz, I. (1971) Experientia 27, 764—765
17 Yunes, R., Goldhammer, A.R., Garner, W.K. and Cordes, E.H. (1977) Arch. Biochem. Biophys. 183, 105—112
18 Dawson, C.R., Drake, A.F., Helliwell, J. and Hider, R.C. (1978) Biochim. Biophys. Acta 510, 75—86
19 De Bony, J., Dufourcq, J. and Clin, B. (1979) Biochim. Biophys. Acta 552, 531—534
20 Drake, A.F. and Hider, R.C. (1979) Biochim. Biophys. Acta 555, 371—373
21 Brown, L.R. (1979) Biochim. Biophys. Acta 557, 135—148
22 Lauterwein, J., Brown, L.R. and Wuethrich, K. (1980) Biochim. Biophys. Acta 622, 219—230
23 Brown, L.R., Lauterwein, J. and Wuethrich, K. (1980) Biochim. Biophys. Acta 622, 231—244
24 Schoch, P., Sargent, D.F. and Schwyzer, R. (1979) J. Membrane Biol. 46, 71—89
25 McLaughlin, S. (1977) in Current Topics in Membranes and Transport (Bronner, F. and Kleinzeller, A., eds.), Vol. 9, pp. 71—144, Academic Press, New York
26 Aveyard, R. and Haydon, D.A. (1973) An Introduction to the Principles of Surface Chemistry, Cambridge University Press, London
27 Barlow, C.A. and MacDonald, J.R. (1967) Adv. Electrochem. Electrochem. Eng. 6, 1—199
28 Brown, R.H. (1974) Prog. Biophys. Mol. Biol. 28, 341—370
29 Singleton, W.S., Gray, M.S., Brown, M.L. and White, J.L. (1965) J. Am. Oil Chem. Soc. 42, 53—56
30 King, T.P., Sobotka, A.K., Kochoumian, L. and Lichtenstein, L.M. (1976) Arch. Biochem. Biophys. 172, 661—671
31 Montal, M. and Mueller, P. (1972) Proc. Natl. Acad. Sci. U.S.A. 69, 3561—3566
32 Faucon, J.F., Dufourcq, J. and Lussan, C. (1979) FEBS Lett. 102, 187—190
33 Mollay, C. (1976) FEBS Lett. 64, 65—68
34 Strom, R., Crifo, C., Viti, V., Guidoni, L. and Podo, F. (1978) FEBS Lett. 96, 45—50
35 Wada, A. (1976) Adv. Biophys. 9, 1—63
36 Wang, C.-C. and Brunner, L.J. (1978) Biophys. J. 24, 749—764
37 Anderson, O.S., Feldberg, S., Nakadomari, H., Levy, S. and McLaughlin, S. (1978) Biophys. J. 21, 35—70
38 Meyer, S.L. (1975) Data Analysis for Scientists and Engineers, Chapter 32. John Wiley and Sons, Inc., New York